Classical Liénard equations of degree $n \geq 6$ can have $[\frac{n-1}{2}] + 2$ limit cycles

P. De Maesschalck[☆], F. Dumortier

Hasselt University, Campus Diepenbeek, Agoralaan gebouw D, B-3590 Diepenbeek, Belgium

Abstract

Based on geometric singular perturbation theory we prove the existence of classical Liénard equations of degree 6 having 4 limit cycles. It implies the existence of classical Liénard equations of degree $n \geq 6$, having at least $[\frac{n-1}{2}] + 2$ limit cycles. This contradicts the conjecture from Lins, de Melo and Pugh formulated in 1976, where an upperbound of $[\frac{n-1}{2}]$ limit cycles was predicted. This paper improves the counterexample from Dumortier, Panazzolo and Roussarie (2007) by supplying one additional limit cycle from degree 7 on, and by finding a counterexample of degree 6. We also give a precise system of degree 6 for which we provide strong numerical evidence that it has at least 3 limit cycles.

Keywords: slow-fast system, singular perturbations, limit cycles, relaxation oscillation, classical Liénard equations
2000 MSC: 37G15, 34E17, 34C07, 34C26

1. Introduction

The so-called Hilbert-Smale problem ([1], 13th problem) asks for the maximum number of limit cycles that classical Liénard equations can have, depending on the degree. A scalar second-order differential equation

$$\ddot{x} + f(x)\dot{x} + x = 0$$

can be studied in a phase plane as a system

$$\left\{ \begin{array}{rcl} \dot{x} & = & y \\ \dot{y} & = & -x - f(x)y, \end{array} \right. \tag{1}$$

or in the so-called Liénard plane as

$$\left\{ \begin{array}{rcl} \dot{x} & = & y - F(x) \\ \dot{y} & = & -x, \end{array} \right. \tag{2}$$

[☆]Postdoctoral researcher of the Research Foundation FWO Flanders
Email addresses: peter.demaesschalck@uhasselt.be (P. De Maesschalck[☆]), freddy.dumortier@uhasselt.be (F. Dumortier)

where $F(x) = \int_0^x f(s)ds$. The systems (1) and (2) are analytically conjugate and are both called *classical Liénard equations*. The degree of the Liénard equation is given by the degree of F. The number of limit cycles of such Liénard equations can be studied in either form (1) or (2).

In 1976 (see [2]), A. Lins, W. de Melo and C. Pugh conjectured that the maximum number of limit cycles for a classical Liénard equation of degree n would be equal to $[\frac{n-1}{2}]$ (the largest integer less than or equal to $\frac{n-1}{2}$), inducing the occurrence of at most 2 limit cycles in degree 6 and 3 limit cycles in degree 7. It was not too hard to understand that the conjecture seemed very reasonable. Up to affine changes in (x, y, t), including a time reversal if necessary, one can write the function F in system (2) as

$$F(x) = x^{2\ell} + \sum_{i=1}^{2\ell-1} a_i x^i, \tag{3}$$

in case $n = 2\ell$, or

$$F(x) = x^{2\ell+1} + \sum_{i=1}^{2\ell} a_i x^i, \tag{4}$$

in case $n = 2\ell + 1$. Systems (2) with a function F as in (3) represent (time-reversible) centers when all a_i, with i odd, are zero. Let us write these a_i as $(a_1, a_3, \ldots, a_{2\ell-1})$. There are ℓ such parameters and they represent "rotational parameters" (see e.g. [3]), in the sense that if one only changes one of them, for example a_{2j+1}, in expression (3), then the determinant

$$\begin{vmatrix} y - \left(x^{2\ell} + \sum\limits_{\substack{i=1 \\ i\neq 2j-1}}^{2\ell-1} a_i x^i + \tilde{a}_{2j-1} x^{2j-1} \right) & y - \left(x^{2\ell} + \sum\limits_{i=1}^{2\ell-1} a_i x^i \right) \\ -x & -x \end{vmatrix}$$

is given by $(\tilde{a}_{2j-1} - a_{2j-1})x^{2j}$, which has everywhere the same sign as $\tilde{a}_{2j-1} - a_{2j-1}$, except for $x = 0$.

In the presence of only one such parameter it clearly follows that system (2) has no limit cycles. It could be expected that at most $\ell - 1$ limit cycles could be created under the influence of all $(a_1, \ldots, a_{2\ell-1})$. Some people even claimed in the literature to have proven this conjecture based on the "rotational properties" of these parameters. In any case it looked like a good strategy to try to work along these lines, at least for $n = 2\ell$.

However, in [4] has been proven the existence of classical Liénard equations of degree 7 with at least 4 limit cycles. This easily implied the existence of classical Liénard equations of degree n, $n \geq 7$, with $[\frac{n-1}{2}] + 1$ limit cycles. The counterexamples were proven to occur in systems

$$\begin{cases} \dot{x} &= y - \left(x^7 + \sum_{i=2}^{6} c_i x^i \right) \\ \dot{y} &= \epsilon(b - x) \end{cases} \tag{5}$$

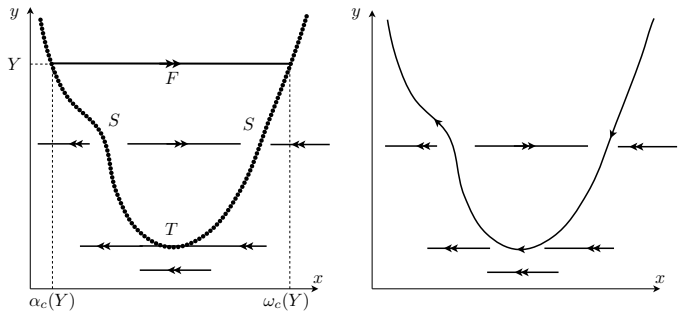

Figure 1: To the left: The dynamics of the layer equation and a FSTS cycle. To the right: the fast dynamics, combined with the slow dynamics on the slow curve

for small $\epsilon > 0$. By affine coordinate changes in (x, y, t), systems (5) can be written as (2), with F as in (4), but for large values of $\|a\|$ with $a = (a_1, \ldots, a_{2\ell})$. For more information, see [5] or [6].

System (5) represents a singular perturbation problem. In [4] the parameters $(c_1, \ldots, c_6)$ were chosen in a way that the function $x^7 + \sum_{i=2}^{6} c_i x^i$ had 6 critical points, permitting to use the results of [7]. The calculations were quite involved and, as far as we know, no one yet succeeded in finding specific numerical examples exhibiting 4 limit cycles.

In [8], among other results, one can find a study of systems

$$\left\{ \begin{array}{rcl} \dot{x} & = & y - \left(x^{2\ell} + \sum_{i=2}^{2\ell-1} c_i x^i \right) \\ \dot{y} & = & \epsilon(b - x) \end{array} \right. \tag{6}$$

in which the c_i are such that the function $x^{2\ell} + \sum_{i=2}^{2\ell-1} c_i x^i$ has only one critical point, let us say a minimum. This leads to the simplest possible degenerate limit periodic sets, from which it is known how to perturb a lot of limit cycles. A degenerate lps (limit periodic set) for a "layer equation", as represented by (6) with $\epsilon = 0$, is a closed curve consisting of fast orbits and parts of the *slow curve* $\{y = x^{2\ell} + \sum_{i=2}^{2\ell-1} c_i x^i\}$; we also call them slow-fast cycles.

In this paper, we will restrict to the type of slow-fast cycles as represented in Figure 1, that we call a FSTS-cycle (fast–slow–turning point–slow). Also [8] dealt with such FSTS-cycles, although represented in the phase plane as in (1) instead of in the Liénard plane as in (2), as we will do here. The slow curves that we will encounter in this paper can and will have inflection points, but no extra critical points besides the one at the origin.

Limit cycles of system (6) that are Hausdorff close to a FSTS-cycle as in Figure 1 are relaxation oscillations, in the sense that the speed close to the fast orbit is of order $O(1)$, while the speed near the slow curves is of order $O(\epsilon)$. The relaxation oscillation itself is of size $O(1)$.

In [8] we succeeded in finding such relaxation oscillations of high multiplicity, together with a complete unfolding. We did however not obtain new counter examples to the [2]-conjecture, but could only check the predicted maximum.

The construction was based on the use of the "*slow divergence integral*", whose definition we will recall now.

Consider a slow-fast family of vector fields

$$\left\{ \begin{array}{rcl} \dot{x} & = & y - H(x,c) \\ \dot{y} & = & \epsilon(b-x) \end{array} \right. \tag{7}$$

with $H(x,c) = x^{2\ell} + \sum_{i=2}^{2\ell-1} c_i x^i$, under the condition that the slow curve $\{y = H(x,c)\}$ is like in Figure 1: we more precisely require that $h(x,c)/x > 0$ (both for $x \neq 0$ and for $x = 0$), where $h(x,c) = \frac{\partial H}{\partial x}(x,c)$. For some $c \sim c_0$ and $x \in [x_0', x_0]$ with $x_0' < 0 < x_0$, we can e.g. parameterize the FSTS-cycles by the value Y at which the fast orbits cut the y-axis. This fast orbit has a specific ω-limit $(\omega_c(Y), H_c(\omega_c(Y)))$ and α-limit $(\alpha_c(Y), H_c(\alpha_c(Y)))$ on the slow curve $\{y = H_c(x) := H(x,c)\}$. The FSTS-cycle Γ_Y^c is defined, for a value c, by the fast orbit through $(0,Y)$ together with the parts of the slow curve in between $x = \omega_c(Y)$ and $x = \alpha_c(Y)$.

Away from the slow curve (i.e. the singular points of (7) for $\epsilon = 0$), the ϵ-perturbation in (7) does not play an important role, and the dynamics in (7) can be studied by examining the fast system (e.g. the unperturbed system for $\epsilon = 0$). Close to the slow curve however, the ϵ-perturbation becomes more relevant. Writing $y = H(x,c) + O(\epsilon)$, and imposing a dynamics along this graph in (7) yields $(h(x,c) + O(\epsilon))x' = \epsilon(b-x)$. The *slow dynamics* is defined as the leading-order approximation of this dynamical system. For (7), the "*slow dynamics*" on the slow part of Γ_Y^c is hence given by

$$x' = -\frac{x}{h(x,c)}$$

and is strictly negative under the assumptions we imposed. This shows that for $\epsilon > 0$ small, orbits of (7) are first attracted to the right branch of Γ_Y^c (following the fast dynamics), and then slowly drift to the left along the slow curve (following the slow dynamics).

In the forthcoming analysis, the divergence integral along closed orbits of (7) reveals to be important, as it gives information on the nature of the closed orbit with respect to its repelling or attracting properties. In a slow-fast context, orbits spend much more time close to the slow curve than away from the slow curve, and one can show that the leading-order approximation of the divergence integral, after multiplication by ϵ, is given by the so-called *slow divergence integral*. One obtains the slow divergence integral by computing the divergence of the vector field along the slow curve, and integrating this divergence w.r.t. the 1-form induced by the slow dynamics. The slow divergence integral of Γ_Y^c is given by

$$I(Y,c) = \int_{\omega_c(Y)}^{\alpha_c(Y)} \frac{h(x,c)^2}{x} dx. \tag{8}$$

In [8] we worked at values c_0 and cycles $\Gamma_{c_0}^{Y_0}$ for which

$$\frac{\partial I}{\partial c_{2j+1}}(Y_0, c_0) \neq 0, \tag{9}$$

and this for every c_{2j+1} present in the expression of $H(x,c)$.

Condition (9) is almost always satisfied for systems (6) and leads in [8] to the proofs of the proposed results on classical Liénard equations. This condition (9) is like a natural condition to express that the parameter c_{2j+1} remains "rotational" in a uniform way when $\epsilon \to 0$ (or in other words, when $\|a\|$ with $a = (a_1, \ldots, a_{2\ell-1})$ as in (3) tends to infinity).

However, in [8], we also encountered combinations (Y_0, c_0) at which the condition (9) gets violated for all c_{2j+1} present in $H(x,c)$. This is a quite exceptional situation that already occurs for $n = 6$. Investigating such a situation we saw that it is possible for $n = 6$ to encounter values c_0 for which 4 limit cycles can be perturbed from the union of FSTS-cycles $\Gamma^Y_{c_0}$ that are present in the layer equation. We more precisely can prove the following theorem:

Theorem 1. *Given the (ϵ, δ, b)-family of polynomial Liénard equations of degree 6*

$$\left\{ \begin{array}{rcl} \dot{x} & = & y - \left(\frac{1}{2}x^2 + 5\delta x^3 - \frac{35}{46}x^4 - 12\delta x^5 + \frac{21}{46}x^6\right) \\ \dot{y} & = & \epsilon(b - x), \end{array} \right. \tag{10}$$

and given $k \in \{1,2,3,4\}$, there exists a smooth curve

$$b = \epsilon \mathcal{B}_k(\epsilon, \delta),$$

defined for $\epsilon \in [0, \epsilon_0]$ and $\delta \in [-\delta_0, \delta_0]$ (for some sufficiently small $\epsilon_0 > 0$ and $\delta_0 > 0$), along which the vector field (10) has exactly k limit cycles when $\delta \neq 0$ and $\epsilon \in]0, \epsilon_1(\delta)]$ for some $\epsilon_1 \colon [-\delta_0, \delta_0] \to \mathbf{R}$ with $\epsilon_1(\delta) > 0$ for $\delta \neq 0$. All these limit cycles are hyperbolic and surround a hyperbolic focus that is attracting when $\delta < 0$ and repelling when $\delta > 0$.

The proof of Theorem 1 will be given in Section 2. For $\delta \sim 0$, $\delta \neq 0$, the limit cycles obtained in Theorem 1 are relaxation oscillations that tend towards specific slow-fast cycles Γ_{Y_i}, $i = 1, \ldots, k$, when $\delta \to 0$. We will show that the heights Y_i of these slow-fast cycles are located inside a compact interval $[Y_{\min}, Y_{\max}]$ that does not depend on (ϵ, δ) and that is bounded away from 0. Hence, the canard cycles are relaxation oscillations of size $O(1)$.

As usual in that kind of construction we can take ϵ_1 to be a smooth function on $[-\delta_0, \delta_0]$ with $\epsilon_1(0) = 0$. We can also remark that the functions $\mathcal{B}_k$ are in no way unique. In fact, for every $k \in \{1,2,3,4\}$, there is an infinity of such curves. More precise information can be found in Section 2.2.

Let $(\epsilon, \delta, b) = (\epsilon_0, -\nu_0, b_0)$ be fixed and let

$$\left\{ \begin{array}{rcl} \dot{x} & = & y - H(x, \nu_0) \\ \dot{y} & = & \epsilon_0(b_0 - x), \end{array} \right. \tag{11}$$

with $H(x, \nu_0) = \frac{1}{2}x^2 - 5\nu_0 x^3 - \frac{35}{46}x^4 + 12\nu_0 x^5 + \frac{21}{46}x^6$, represent a system with 4 hyperbolic limit cycles, of which the largest one is attracting (hence with $\nu_0 > 0$). If we change $H(x, \nu_0)$ in (11) by $H(x, \nu_0) + \nu_1 x^7$, for ν_1 sufficiently small, then the four limit cycles persist. Moreover, by taking $\nu_1 < 0$, the circle

at infinity will be attracting (see e.g. [9]) and the new system of degree 7 will have at least 5 limit cycles of odd multiplicity. Fixing such $\nu_1 < 0$, $\nu_1 \sim 0$, and considering $H(x, \nu_0) + \nu_1 x^7 + \nu_2 x^8$ with ν_2 sufficiently small, will give a system of degree 8 with at least 5 limit cycles of odd multiplicity. Continuing this way by adding $\nu_j x^j$, for $j \geq 9$, with ν_j decreasing sufficiently fast, and taking care of alternating the signs of the ν_j with j odd, one easily obtains following result:

Theorem 2. *Let $n \geq 6$. There exist polynomial vector fields of degree n of the form (2) with at least $\left[\frac{n-1}{2}\right] + 2$ hyperbolic limit cycles.*

Typically, the canard cycles obtained in Theorem 1 are very hard to find numerically, even in the very specific setting of Theorem 1. The reason is the singular nature of slow-fast systems like (10): all orbits through $\{x = 0\}$, and with a y-coordinate between $[Y_{\min}, Y_{\max}]$, with $0 < Y_{\min} < Y_{\max}$, will follow a fast–slow trajectory in forward time, until they intersect $\{x = 0\}$ again somewhere close to the turning point. Similarly, these orbits will follow a fast–slow trajectory in negative time, until they intersect $\{x = 0\}$. In other words, one can define a "forward map" and a "backward map", and the periodic orbits are then identified as the zeros of the difference between the forward and backward map. In a singular perturbation context, the image of the interval $[Y_{\min}, Y_{\max}]$ under the forward map is an interval of exponentially small size ($O(\exp(-\kappa/\epsilon))$ for some $\kappa > 0$). The image of the backward map is an interval of a similar size. This implies that in order to distinguish periodic orbits from orbits that are not periodic, one needs an accuracy of the order $O(\exp(-\kappa/\epsilon))$.

The constant κ in the exponential expression can be determined and is related to the one-sided slow divergence integral (the slow divergence integral as in (8), but taken between the ω-limit and the turning point at $x = 0$ instead of between ω and α), since this measures the amount of attraction the forward orbit undergoes. This immediately implies that the bigger the canard-cycle is, the more difficult it is to find it numerically. Of course, taking the singular parameter ϵ larger, the exponential estimates become more tractable and this would increase the hope to find bigger canards. However, the larger ϵ, the less guarantee one has that the limit cycles appear as claimed in Theorem 1.

After the publication of [4] different people expressed their interest in seeing a numerical example of a Liénard equation with more limit cycles than conjectured in [2]. In an appendix, we come up with an example, close to the example predicted by Theorem 1. We find 3 limit cycles fixing ϵ at 0.005. The example with 3 limit cycles is already a numerical counterexample to the conjecture of [2] for degree 6.

2. Proof of Theorem 1

The proof of Theorem 1 relies on several ingredients. We first show that there is a compact annulus around the origin where the vector field (10) has k limit cycles, for $0 < \epsilon \leq \epsilon_0$, $0 < |\delta| \leq \delta_0$ and $k = 1, 2, 3, 4$. We then show that the result holds in any compact annulus around the origin. Next, we

show that we can extend the annulus towards infinity (using Poincaré-Lyapunov compactification), and finally, we show that no additional limit cycles are found near the origin. Of course, to obtain lower bounds for the number of limit cycles, only the first part of the proof is essential. The study near the origin and near infinity is included to show that the techniques that we use permit to treat the systems under consideration completely.

In the first part of the proof, we study the slow divergence integral, as defined in Section 1. A result from [10] shows that a slow-fast system where the slow divergence integral has ℓ simple zeros can lead to $\ell + 1$ limit cycles. Because it is an essential ingredient in our proof, we will repeat this result here, together with a well-known result on the entry–exit relation in slow-fast systems. This is done in Section 2.1. In Section 2.2, we show that the slow divergence integral of (10) has exactly 3 zeros when $\delta \neq 0$, $\delta \sim 0$. In Section 2.3, we finish the proof of Theorem 1 by combining the information from previous subsections with information near the origin and near infinity.

2.1. Essential ingredients from geometric singular perturbation theory

We consider

$$\left\{ \begin{array}{rcl} \dot{x} & = & y - H(x,c) \\ \dot{y} & = & \epsilon(b-x) \end{array} \right. \tag{12}$$

where $H(x,c) = \int_0^x h(s,c)ds$ and $h(x,c)/x > 0$ for all x. Given a height Y, we consider the slow-fast cycle Γ_Y^c as defined in the introduction. Recall the x-coordinates $\alpha_c(Y)$, $\omega_c(Y)$ of the fast part of the slow-fast cycle.

Proposition 1. *(e.g. [11]) There is a smooth surface $b = \epsilon\mathcal{B}_Y(\epsilon,c)$, defined for $\epsilon \in [0,\epsilon_0]$, with $\epsilon_0 > 0$ sufficiently small, along which (12) has an (ϵ,c)-family of periodic orbits intersecting the y-axis at height Y. The periodic orbits tend towards Γ_Y^c as $\epsilon \to 0$. When $I(Y,c) \neq 0$, the family of periodic orbits are, for $\epsilon > 0$, hyperbolic limit cycles (attracting or repelling, depending on whether the sign of $I(Y,c)$ is negative or positive).*

This proposition can be used to fix one limit cycle of a prescribed size. We will restrict to choices of a height Y where $I(Y,c) \neq 0$. We then define the related *entry–exit relation*. To that end, we consider a situation where we have a hyperbolic limit cycle along a given surface $b = \epsilon\mathcal{B}_Y(\epsilon,c)$, as specified in Proposition 1. We assume that $I(Y,c) < 0$; the other case can be reduced to this case after applying $(x,t) \mapsto (-x,-t)$.

We introduce the *slow-relation function*: A pair (Y_a, Y_r) satisfies the slow relation when

$$\int_{\omega_c(Y_a)}^{\alpha_c(Y_r)} \frac{h(x,c)^2}{x} dx = 0.$$

For each $Y_a > 0$ there exists a unique Y_r so that (Y_a, Y_r) satisfies the slow relation and vice versa.

Proposition 2. *(Entry–exit relation) Fix (Y,c) for which $I(Y,c) < 0$, and fix a compact interval $[Y_{min}, Y_{max}]$ containing Y in its interior. Consider the vector*

field (12) along the parameter surface specified in Proposition 1. Then, there is a $0 < \tilde{Y}_{min} < Y_{min}$ *so that for* $\epsilon > 0$ *small enough, the first return map*

$$P_{\epsilon,c} \colon \{0\} \times [Y_{min}, Y_{max}] \to \{0\} \times [\tilde{Y}_{min}, Y_{max}]$$

is well-defined. The first return map is continuous as $\epsilon \to 0$*, and tends towards a piecewise-analytic map* $P_{0,c}$ *defined as follows:*

1. $P_{0,c}(Y') \equiv Y$ *for all* $Y' \geq Y_a$ *where* $Y_a < Y$ *is the unique height for which* (Y, Y_a) *satisfy the slow relation.*
2. $P_{0,c}(Y') = Y'_r$ *for all* $Y' < Y_a$ *where* Y'_r *is the unique height for which* (Y'_r, Y') *satisfy the slow relation.*

This Proposition is a direct consequence of the results in [11], where a more elaborated entry–exit relation is given. From this Proposition, we can deduce that there will be no limit cycles with height in $]Y, Y_{\max}]$. Furthermore, given a height $Y' < Y$ for which $I(Y, c) \neq 0$, then the result on the Poincaré map at height Y shows that the orbit is either spiraling upwards ($I < 0$) or spiraling downwards ($I > 0$). It indicates that additional limit cycles are only to be expected at heights where the slow divergence integral is zero. This is essentially the topic of the next Proposition:

Proposition 3. *[10] Consider system (12) along a parameter surface* $b = \epsilon \mathcal{B}_Y(\epsilon, c)$ *as provided in Proposition 1. If for some* $c = c_*$*, the slow divergence integral* $I(Y, c_*)$ *has a simple zero at* $y = Y_* \in]0, Y[$*, then there exists a Hausdorff neighborhood* V *around* $\Gamma^{c_*}_{Y_*}$*, such that for* $\epsilon > 0$ *small enough and for* c *close enough to* c_**, the vector field (12) with* $b = \epsilon \mathcal{B}_Y(\epsilon, c)$ *has a unique limit cycle in* V*. If* $\frac{\partial I}{\partial Y}(Y_*, c_*) > 0$ *then the limit cycle is hyperbolically attracting, if* $\frac{\partial I}{\partial Y}(Y_*, c_*) < 0$*, then the limit cycle is hyperbolically repelling.*

In the next section, we focus on providing an example of a slow-fast vector field, having a slow divergence integral with 3 zeros.

2.2. Slow divergence integrals with 3 *zeros*

We consider a family of vector fields

$$\begin{cases} \dot{x} &= y - F(x, c) \\ \dot{y} &= \epsilon(b_0 - x), \end{cases}$$

where $c = (a_0, a_1, b_1, b_2)$, $\epsilon \geq 0$, and b_0 is a parameter close to 0. We write

$$F(x) = F(x, c) = \int_0^x f(s) ds,$$
$$f(x) = f(x, c) := x + b_1 x^3 + b_2 x^5 + a_0 x^2 + a_1 x^4.$$

The parameters $c = (a_0, a_1, b_1, b_2)$ will be chosen very specifically later, but we prefer to keep them general for the moment; we however keep $(a_0, a_1) \sim (0, 0)$. For $(a_0, a_1) = (0, 0)$, the family of vector fields is symmetric w.r.t. $(x, t) \mapsto$

$(-x,-t)$. Hence, (b_1,b_2) are parameters that preserve symmetry, whereas the parameters (a_0,a_1) are symmetry-breaking. We will choose (b_1,b_2) so that

$$\frac{f(x,0,0,b_1,b_2)}{x}>0, \qquad \forall x,$$

and hence so that $f(x,a_0,a_1,b_1,b_2)/x>0$ on the entire real line, when (a_0,a_1) is sufficiently close to $(0,0)$. This ensures that the shape of $y=F(x,c)$ is like in Figure 1, and on the other hand it also ensures that the slow dynamics $x'=-x/f(x)$ is regular. Recall that a slow-fast cycle Γ^c_Y has a fast horizontal orbit, with an ω-limit on the right branch of the curve $y=F(x)$; its x-coordinate is denoted by $\omega_c(Y)$. The x-coordinate of the α-limit will be denoted $\alpha_c(Y)$. Of course

$$\alpha_c(Y)<0<\omega_c(Y), \qquad F(\alpha_c(Y),c)=Y=F(\omega_c(Y),c).$$

Along this section, it will be convenient to parameterize the slow-fast cycles by the omega-limit $\omega_c(Y)$, instead of by its height Y. We will hence define the slow-fast cycle $\overline{\Gamma}^c_x$, with some $x>0$, as the slow-fast cycle with height $Y=F(x,c)$. The corresponding α-limit will be denoted $\overline{\alpha}_c(x)=\overline{\alpha}(x,c)$. The relation $x\mapsto\overline{\alpha}_c(x)$ is called the *fast relation*. The next proposition examines the asymptotics of the (analytic) fast relation function for (a_0,a_1) near $(0,0)$.

Lemma 1. *The fast relation function is given by*

$$\overline{\alpha}_c(x)=-x+a_0R_0(x,b_1,b_2)+a_1R_1(x,b_1,b_2)+O(\|(a_0,a_1)\|)^2,$$

as $(a_0,a_1)\to(0,0)$*, where*

$$R_0(x,b_1,b_2)=-\frac{2}{3}\frac{x^2}{1+b_1x^2+b_2x^4},$$
$$R_1(x,b_1,b_2)=-\frac{2}{5}\frac{x^4}{1+b_1x^2+b_2x^4}.$$

Proof. Due to the symmetry, we have $\overline{\alpha}(x,0,0,b_1,b_2)\equiv -x$, so it suffices to look at the partial derivatives at $(a_0,a_1)=(0,0)$. This is an elementary calculation based on implicit differentiation of the equation

$$F(\overline{\alpha}(x,a_0,a_1,b_1,b_2),a_0,a_1,b_1,b_2)=F(x,a_0,a_1,b_1,b_2)$$

with respect to a_i, for $i=0,1$. We find $f(\overline{\alpha}_c,c).\frac{\partial\overline{\alpha}_c}{\partial a_i}+\frac{\partial F}{\partial a_i}(\overline{\alpha}_c,c)=\frac{\partial F}{\partial a_i}(x,c)$, implying that

$$((-x)+b_1(-x)^3+b_2(-x)^5).R_i(x,b_1,b_2)=\frac{1}{3+2i}x^{3+2i}-\frac{1}{3+2i}(-x)^{3+2i}.$$

This proves the lemma. □

Let us now compute the slow divergence integral

$$I(x,c)=\int_x^{\overline{\alpha}_c(x)}\frac{f(s,c)^2}{s}ds.$$

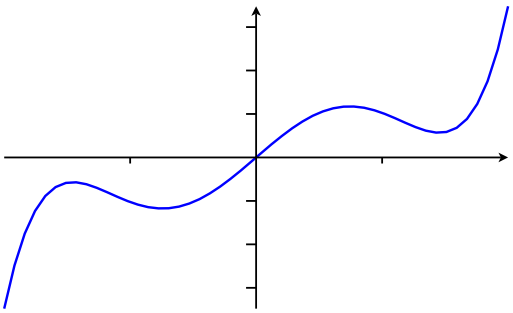

Figure 2: Graph of $f(x, 0, 0, b_1^*, b_2^*)$

Lemma 2. *The slow divergence integral is given by*

$$I(x, a_0, a_1, b_1, b_2) = a_0 I_0(x, b_1, b_2) + a_1 I_1(x, b_1, b_2) + O(\|(a_0, a_1)\|)^2,$$

as $(a_0, a_1) \to (0, 0)$*, where*

$$I_0(x, b_1, b_2) = -\frac{2}{3}x^3 - \frac{2}{15}b_1 x^5 + \frac{2}{21}b_2 x^7,$$
$$I_1(x, b_1, b_2) = -\frac{2}{5}x^5 - \frac{6}{35}b_1 x^7 - \frac{2}{45}b_2 x^9.$$

Proof. Again, a symmetry argument is used to show that $I(x, 0, 0, b_1, b_2) \equiv 0$, so it suffices to look at the partial derivatives w.r.t. a_i. □

As explained in the introduction, we look for parameter values (b_1, b_2) where at a given point, say at $x = 1$, both I_0 and I_1 are zero. We find a unique solution

$$(b_1^*, b_2^*) = (-\tfrac{70}{23}, \tfrac{63}{23}).$$

Observe that $f(x, 0, 0, b_1^*, b_2^*) = \frac{x}{23}(23 - 70x^2 + 63x^4)$ has no zeros, meaning that this choice of function satisfies the condition $f(x)/x > 0$ for all x, see also Figure 2. Let us now, for this specific choice of parameters (b_1^*, b_2^*), look at the linearization of I along the line

$$a_1 = -4a_0.$$

We find

$$\begin{aligned} I(x, a_0, -4a_0, b_1^*, b_2^*) &= \left(\frac{56}{115}x^9 - \frac{42}{23}x^7 + \frac{692}{345}x^5 - \frac{2}{3}x^3\right) a_0 + O(a_0^2) \\ &= \left(\frac{2}{345}x^3(x^2 - 1)(115 - 231x^2 + 84x^4)\right) a_0 + O(a_0^2). \end{aligned}$$

The function $\frac{1}{a_0} I(x, a_0, -4a_0, b_1^*, b_2^*)\Big|_{a0=0}$ has besides the zero $x = 1$, two additional zeros, respectively around $x \approx 0.8$ and $x \approx 1.4$. These three zeros are

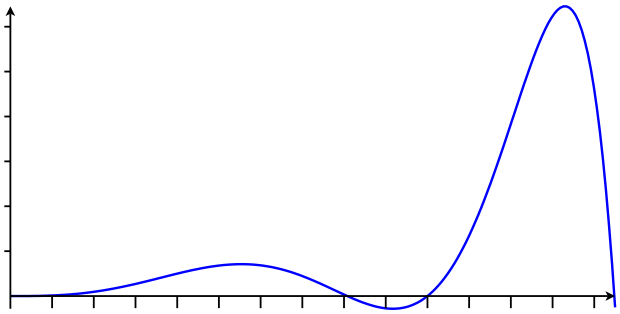

Figure 3: Graph of $\frac{2}{345}x^3(1-x^2)(115-231x^2+84x^4)$, which is the first-order Taylor coefficient (w.r.t. a_0) of $-I(x,c)$ along $c=(a_0,-4a_0,b_1^*,b_2^*)$

simple and hence persist as zeros of the slow divergence integral for $|a_0|$ small, and taking $|a_0|$ small enough, these zeros lie inside the compact interval $\left[\frac{1}{2},2\right]$. Renaming $a_0=15\delta$, we find

$$f(x)=x+15\delta x^2-\frac{70}{23}x^3-60\delta x^4+\frac{63}{23}x^5,$$

which leads to a vector field of the form (10) specified in the formulation of Theorem 1.

Let

$$\frac{1}{2}\leq x_1(\delta)<x_2(\delta)<x_3(\delta)\leq 2$$

be the three zeros of $\frac{1}{a_0}I(x,a_0,-4a_0,b_1^*,b_2^*)\Big|_{a_0=15\delta}$. Of course $x_1(0)$, $x_2(0)$ and $x_3(0)$ are exactly the (positive) zeros of $(x^2-1)(115-231x^2+84x^4)$ (see also Figure 3), and are hence distinct for $\delta\sim 0$. Let $Y_1(\delta)$, $Y_2(\delta)$, $Y_3(\delta)$ be the heights of the corresponding slow-fast cycles.

Now consider the heights $Y^{(1)}=\frac{1}{4}$, $Y^{(2)}$ a height between $Y_1(0)$ and $Y_2(0)$, $Y^{(3)}$ a height between $Y_2(0)$ and $Y_3(0)$, and $Y^{(4)}=3$. We then apply Proposition 1 at all these heights, and find different surfaces $b=\epsilon\mathcal{B}_k(\epsilon,\delta)$ in parameter space, $k=1,2,3,4$. It is then a direct consequence of the entry–exit relation stated in Proposition 2 and Proposition 3 that the family of vector fields (10) along $b=\mathcal{B}_k(\epsilon,\delta)$, and for $\epsilon>0$ small enough and $\delta\neq 0$ close enough to 0, has exactly k limit cycles in any compact annulus around the origin. Furthermore, From Proposition 3 clearly follows that all these limit cycles are hyperbolic.

2.3. Dynamics near the turning point and near infinity

We continue the discussion from previous section, and use the same notations. When $\delta<0$, the sign of I goes from $+$ to $-$, from $-$ to $+$ and from $+$ to $-$ again. This implies that the smallest of the obtained limit cycles along any

of the four surfaces $b = \epsilon \mathcal{B}_k(\epsilon, \delta)$ is always repelling. When $\delta > 0$, it is the other way around.

On the other hand, we know that the four surfaces $b = \epsilon \mathcal{B}_k(\epsilon, \delta)$ all have the same Taylor development w.r.t. ϵ (and are in fact exponentially close to each other). Using formal computations, together with the known situation for $\delta = 0$ and $\epsilon = 0$, it is elementary to check that

$$b = -15\delta\epsilon(1 + O(\epsilon)).$$

This information can be used to see that for $\epsilon > 0$ and $\delta \neq 0$ small enough, the unique singularity of (10) near the origin is repelling when $\delta > 0$ and attracting when $\delta < 0$. Unfortunately, the hyperbolic attraction/repulsion at this point is not obtained uniformly in ϵ, and therefore we need an additional argument to show that in a uniform neighborhood of the origin, system (10) has no limit cycles.

This additional argument is provided in [12] and [13]. We give more details in Section 2.3.1. The behaviour at infinity is studied in Section 2.3.2.

2.3.1. Dynamics near the turning point

We take any $\delta_1 \in [-\delta_0, \delta_0]$ with $\delta_1 \neq 0$. In terms of [12], equation (10), for $\delta \sim \delta_1$, represents a slow-fast Hopf bifurcation of codimension one. The codimension is one because the coefficient in front of $x^3 \frac{\partial}{\partial x}$ is nonzero. In [12], it has been proven that in a uniform neighborhood of the origin in (x, y, ϵ)-space, the equations (10) have at most two limit cycles. In Section 3.1.4 of [13], more precisely in the subsections "Cyclicity of the origin $(\overline{x}, \overline{y}) = (0, 0)$" and "Unicity of the limit cycle near Γ_0", it has been shown, based on [12], that one can in fact have at most one limit cycle in a slow-fast Hopf bifurcation of codimension 1, and it has to be simple.

Assume now $\delta_1 < 0$. We now restrict to $b = \epsilon \mathcal{B}_k(\epsilon, \delta)$ as in the statement of Theorem 1, and denote the limit cycles obtained in Section 2.2 by $L_1, \ldots, L_k$, in increasing order of size. From the observations made above we know that there can be at most one extra limit cycle inside L_1 and it has to be simple. Since $\delta_1 < 0$, we have $b > 0$, and then we know from Section 2.2 that the focus is attracting, while the limit cycle L_1 is repelling. It is hence not possible to have an extra limit cycle inside L_1. A similar argument is possible when $\delta_1 > 0$.

2.3.2. Dynamics near infinity

Remains to show that no limit cycles can appear near infinity. Since we only need to look in the halfplane where $Y > 0$, the relevant coordinate change is given by

$$(x, y) = \left(\frac{X}{u}, \frac{1}{u^6} \right),$$

where $u > 0$ is small and X is kept in a large compact interval. The line $\{u = 0\}$ represents the line at infinity. The family of vector fields

$$\left\{ \begin{array}{rcl} \dot{x} & = & y - \left(\frac{1}{2}x^2 + \frac{1}{3}a_0 x^3 + \frac{1}{4}b_1 x^4 + \frac{1}{5}a_0 x^5 + \frac{1}{6}b_2 x^6 \right) \\ \dot{y} & = & \epsilon(b - x) \end{array} \right.$$

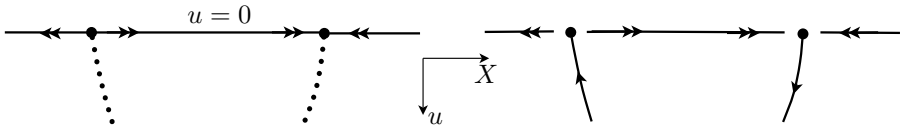

Figure 4: Behaviour at infinity, for $\epsilon = 0$ and for $\epsilon > 0$. The line at infinity is represented by $\{u = 0\}$.

(of which (10) in Theorem 1 is an example) is written in the new coordinates near infinity, after multiplication by u^5, as

$$\begin{cases} \dot{X} &= 1 - \left(\frac{1}{2}u^4X^2 + \frac{1}{3}a_0u^3X^3 + \frac{1}{4}b_1u^2X^4 + \frac{1}{5}a_1uX^5 + \frac{1}{6}b_2X^6\right) \\ & \qquad -\frac{1}{6}\epsilon u^{10}X\left(bu - X\right) \\ \dot{u} &= -\frac{1}{6}\epsilon u^{11}\left(bu - X\right) \end{cases}$$

At the line at infinity $\{u = 0\}$, we find two semi-hyperbolic singularities $\{X = \pm(6/b_2)^{1/6}\}$, under the assumption that $b_2 > 0$ (and this is the case in the example (10)). Define $X_0^{\pm} = \pm(6/b_2)^{1/6}$ and consider center manifolds

$$X = X_0^{\pm} + O(u)$$

at these singularities. It is not hard to find that

$$X = X_0^{\pm} - \frac{a_1}{5b_2}u + O(u^2),$$

at each of these points. This allows us the compute the dynamics inside the center manifold up to leading order. We find, at both points,

$$\dot{u} = \epsilon u^{11}\left(\frac{X_0^{\pm}}{6} + O(u)\right).$$

This behaviour is compatible with the slow dynamics: pointing downwards (increasing u) on the right branch of the slow curve, and pointing upwards on the left branch of the slow curve, see also Figure 4. The two singularities at infinity are hence semi-hyperbolic saddles, and hence have unique ϵ-families of center manifolds.

We denote the unique ϵ-family of center manifolds by $X = \psi^{\pm}(u, \epsilon)$. For $u = u_0$ sufficiently small, we consider a small segment

$$\Sigma_{\mu}\colon \{(X, u)\colon\ -\mu \leq X - \psi^{+}(u_0, \epsilon) \leq \mu, u = u_0\},$$

for some small $\mu > 0$. Any limit cycle that comes near infinity will for sure cross this section (orbits that do not cross this section can be studied in the (x, y)-plane inside a large compact set). From the entry–exit relation in Proposition 2 clearly follows that the orbit of the left end point of Σ_{μ} will make a contour around the unique singularity near the turning point and will cross the section

$\{x = 0\}$ again at a point with a height that is $o(1)$-close to the height of the biggest limit cycle Y_k. Now it is easy to see (with the more elaborate entry–exit relation in [11]) that also the right end point of Σ_μ has this property. This means that *all* orbits through Σ_μ will end up near $(0, Y_k)$, for $\epsilon > 0$ small enough. It clearly follows that no limit cycles near infinity are present, and hence that all limit cycles are the ones that were obtained in Section 2.2.

This concludes the proof of Theorem 1.

Appendix: Finding three canard cycles numerically

As will be explained later in this section, a very high precision is needed to find canards, even for moderately small values of the singular parameter ϵ. The numerical simulations described in this section are based on a Runge-Kutta (order 7) ode-solver, with fixed step size h. Typically, $h = 10^{-6}$ or smaller. The implementation is done in C++, and the tests ran on a regular desktop computer. Because of the very sensitive nature of the dynamics of slow-fast vector fields, some of the calculations are done in quadruple precision. To that end, we use the "double–double" C++ library, implemented by the authors of [14] and publicly available.

Instead of working with (10), it reveals better to work with a slight adaptation

$$\begin{cases} \dot{y} &= y - F^{\#}(x) \\ \dot{x} &= \epsilon(b - x), \end{cases} \tag{13}$$

with

$$\text{with } F^{\#}(x) = \frac{1}{2}x^2 - \frac{1}{100}x^3 - \left(\frac{35}{46} + \frac{1}{16}\right)x^4 + \frac{23}{1000}x^5 + \frac{21}{46}x^6. \tag{14}$$

Let us explain why an adaptation is helpful, and at the same time explain why only 3 limit cycles are searched instead of 4 limit cycles as predicted by Theorem 1.

To understand this, we first consider the theoretical example (10) and notice that it is not possible to choose ϵ very small while computing limit cycles, as the smaller ϵ is chosen, the more digits accuracy are needed in order to distinguish the orbits from each other. Indeed: if one tracks two orbits, starting respectively at $(0, Y_0)$ and at $(0, Y_1)$, with $Y_0 < Y_1$, then both orbits will intersect $\{x = 0\}$ again somewhere slightly below the fixed point at heights $T(Y_0)$, $T(Y_1)$. From singular perturbation theory, it is clear that $|T(Y_0) - T(Y_1)| = O(\exp(I_-(Y_0)/\epsilon))$, where I_- is the "one-sided slow divergence integral"

$$I_-(Y) = \int_{\omega(Y)}^{0} \frac{f(x)^2}{x} dx < 0,$$

calculated along the relevant part of the attracting branch of the slow curve. This means that in order to distinguish the orbit through $(0, Y_0)$ from the orbit through $(0, Y_1)$, one needs $O(|I_-(Y_0)|/\epsilon)$ digits accuracy. Therefore, by choosing

$\epsilon = O(10^{-4})$, it is unlikely that trustworthy results will be found with numerical analysis.

The same argument shows that it is very difficult to find 4 limit cycles of (10), even with more moderate choices of ϵ: recall the positions $x_1(\delta)$, $x_2(\delta)$, $x_3(\delta)$ of the zeros of the slow divergence integral from Section 2.2. Let Y_i, $i = 1, 2, 3$, be the related heights of the slow-fast cycles, then for $\delta = 0$ we have

$$\begin{aligned} &x_1 \approx 0.81, && Y_1 \approx 0.13, && I_-(Y_1) \approx -0.072; \\ &x_2 \approx 1.00, && Y_2 \approx 0.20, && I_-(Y_2) \approx -0.101; \\ &x_3 \approx 1.45, && Y_3 \approx 1.91, && I_-(Y_3) \approx -7.140. \end{aligned}$$

showing that for $\epsilon = 0.01$,

$$\begin{aligned} &\exp(-I_-(Y_1)/\epsilon) = O(10^{-4}), \\ &\exp(-I_-(Y_2)/\epsilon) = O(10^{-5}), \\ &\exp(-I_-(Y_3)/\epsilon) = O(10^{-310}). \end{aligned} \tag{15}$$

This shows that the region in phase space where the third zero of the slow divergence integral becomes relevant in the analysis, is completely out of reach from a numerical point of view. Even with moderate values of ϵ and δ, for example with $\epsilon = 0.1$ and $\delta = 0.001$, we find that $\exp(I_-(Y_3)/\epsilon) = O(10^{-31})$, which would require an accuracy far beyond the capabilities of standard desktop computers.

In the remainder of this section, we will hence limit to finding 3 limit cycles, which involves dealing with 2 zeros of the slow divergence integral. But even finding 3 limit cycles for (10) proves to be very difficult, despite of the reasonable required accuracy of the order shown in (15). The explanation can be found in Figure 5, where the *computed* divergence integral is drawn for several values of ϵ. Let us first explain how we have computed these graphs: we consider orbits through $(0, Y)$, and follow them numerically until they reach the section $\{x = 0\}$ once more. We do this both in forward and in backward time. In this computation, we take $b = 0$ (b is in fact $O(\epsilon\delta)$, so can be assumed small and relatively irrelevant in this computation).

Figure 5 shows that although the zeros of the slow divergence integral persist as zeros of the computed integrals, both shift to the right as ϵ increases, the largest one even quite fast. Now it is important to realize that while the x-coordinate of the zero increases, it becomes more and more difficult to deal with limit cycles of that order, as explained before.

Because the zeros of the computed divergence integrals shift to the right too quickly, we consider (13) instead of (10), precisely to keep the zeros of the computed divergence integral sufficiently close to the theoretical values. The vector field (13) is found experimentally in the neighborhood of (10), and has the property that the divergence integral $I(Y)$, for a fixed value of $\epsilon > 0$, has two zeros that have not shifted to the right too much, and where one hence may expect 3 numerically distinguishable limit cycles to appear.

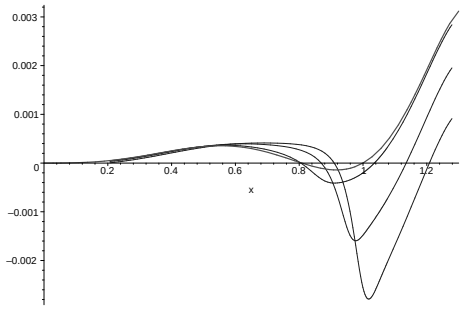

Figure 5: Computed divergence integrals in (10), with $\delta = -0.01$ and for specific choices of ϵ: $\epsilon = 0.001$, $\epsilon = 0.005$, $\epsilon = 0.01$. The thicker curve is δ times the graph in Figure 3. As ϵ increases, the zeros of the divergence integral shift to the right. All curves have an additional zero in $\{x > 1.2\}$, but this part of the graph has not been plotted.

We thus consider (13) for the specific value of $b = 0.000063032171696$. The numerical proof for the existence of the 3 limit cycles is based on the presence of 4 sign changes in the numerical study of the difference map (map in forward time from $\{x = 0\}$ to $\{x = 0\}$ versus map in backward time). This computation is done with very high precision: we used a Runge-Kutta method of order 7, with a step size $h = 10^{-8}$. We find sign changes near heights Y_1, Y_2, Y_3, where $Y_1 \approx 0.25$, $Y_2 \approx 0.21$, and $Y_3 \approx 0.02$. This means that limit cycles of approximately these 3 heights are numerically found. The limit cycles of heights Y_1 and Y_2 are related to the zeros of the slow divergence integral, as indicated by Proposition 3, whereas the limit cycle of height Y_3 is purely related to the specific choice of the parameter b, as indicated by Proposition 1. In fact, we have computed b precisely to have a limit cycle at this specific height.

The first limit cycle, i.e. the cycle near height Y_1, is found with moderate accuracy, say with a step size $h = 10^{-6}$. The second and third limit cycle require a much smaller step size: the computation in that region has been done with step size $h = 10^{-8}$.

Remark. Slight adaptations of the parameter b, or lower accuracy computations will only show 0, 1 or 2 limit cycles. This is due to the fact that all curves $b = \epsilon \mathcal{B}_Y(\epsilon)$, defined in Proposition 1, lie exponentially close to each other. A slight change in b will most probably imply that this value of b lies on a curve $b = \epsilon \mathcal{B}_Y(\epsilon)$ with a height Y less than Y_3. From the entry–exit relation described in Proposition 2 follows that no limit cycles are seen above height Y.

References

[1] S. Smale, Mathematical problems for the next century, in: Mathematics: frontiers and perspectives, Amer. Math. Soc., Providence, RI, 2000, pp. 271–294.

[2] A. Lins, W. de Melo, C. C. Pugh, On Liénard's equation, in: Geometry and topology (Proc. III Latin Amer. School of Math., Inst. Mat. Pura Aplicada CNPq, Rio de Janeiro, 1976), Springer, Berlin, 1977, pp. 335–357. Lecture Notes in Math., Vol. 597.

[3] F. Dumortier, J. Llibre, J. Artés, Qualitative theory of planar differential systems, Universitext, Springer-Verlag, Berlin, 2006.

[4] F. Dumortier, D. Panazzolo, R. Roussarie, More limit cycles than expected in Liénard equations, Proc. Amer. Math. Soc. 135 (6) (2007) 1895–1904 (electronic). doi:10.1090/S0002-9939-07-08688-1.

[5] R. Roussarie, Putting a boundary to the space of Liénard equations, Discrete Contin. Dyn. Syst. 17 (2) (2007) 441–448.

[6] F. Dumortier, Compactification and desingularization of spaces of polynomial Liénard equations, J. Differential Equations 224 (2) (2006) 296–313. doi:10.1016/j.jde.2005.08.011.

[7] F. Dumortier, R. Roussarie, Canard cycles and center manifolds, Mem. Amer. Math. Soc. 121 (577) (1996) x+100, with an appendix by Li Chengzhi.

[8] P. De Maesschalck, F. Dumortier, Bifurcations of multiple relaxation oscillations in polynomial Liénard equations, Proc. Amer. Math. Soc, available online. doi:10.1090/S0002-9939-2010-10610-X.

[9] F. Dumortier, C. Herssens, Polynomial Liénard equations near infinity, J. Differential Equations 153 (1) (1999) 1–29.

[10] F. Dumortier, Slow divergence integral and balanced canard solutions, Qual. Theory of Dyn. Syst. To appear.

[11] P. De Maesschalck, F. Dumortier, Time analysis and entry-exit relation near planar turning points, J. Differential Equations 215 (2) (2005) 225–267. doi:10.1016/j.jde.2005.01.004.

[12] F. Dumortier, R. Roussarie, Birth of canard cycles, Discrete Contin. Dyn. Syst. Ser. S 2 (4) (2009) 723–781. doi:10.3934/dcdss.2009.2.723.

[13] P. De Maesschalck, F. Dumortier, Slow-fast Bogdanov-Takens bifurcations, Journal of Differential Equations 250 (2) (2011) 1000–1025. doi:10.1016/j.jde.2010.07.022.

[14] Y. Hida, X. S. Li, D. H. Bailey, Algorithms for quad-double precision floating point arithmetic, 15th IEEE Symposium on Computer Arithmetic, IEEE Computer Society (2001) 155–162.